

Growth of GaSb-rich and InAs-rich GaInAsSb alloys on GaSb substrates by MOCVD

YONGQIANG NING, TIANMING ZHOU, BAOLIN ZHANG, HONG JIANG,
SHUWEI LI, GUANG YUAN, YUAN TIAN, YIXIN JIN

*Changchun Institute of Physics, Chinese Academy of Sciences, 1 Yan'an Rd., Changchun,
Changchun 130021, People's Republic of China*
E-mail: snmocvd@public.cc.jl.cn

MOCVD growth and characterization of GaSb-rich and InAs-rich GaInAsSb on GaSb substrates was investigated. The surface of InAs-rich GaInAsSb epilayers showed morphological features very different from those on GaSb-rich films. Solid compositions of $\text{Ga}_{1-x}\text{In}_x\text{As}_y\text{Sb}_{1-y}$ films were dependent on growth temperature and the input source ratios, such as Ga/III ratio and Sb/V ratio. Unintentionally doped InAs-rich GaInAsSb showed n-type conduction, and GaSb-rich samples were p-type. A room temperature electron mobility of $5000 \text{ cm}^2 \text{ v}^{-1} \text{ s}^{-1}$ with electron concentration of $3.6 \times 10^{17} \text{ cm}^{-3}$ for InAs-rich films was obtained. On the other hand, a hole mobility of $360 \text{ cm}^2 \text{ v}^{-1} \text{ s}^{-1}$ with a hole concentration of $1 \times 10^{17} \text{ cm}^{-3}$ for GaSb-rich samples was achieved. © 1998 Chapman & Hall

1. Introduction

III-V antimonide compounds are attracting great interest for their applications, such as optical communication, environmental protection, remote sensing of the atmosphere and infrared focal plane arrays for imaging. The room temperature band gap of Sb-contained materials covers the extremely wide range from 1.43 eV to 0.1 eV, corresponding to 0.9 μm to 12 μm . Lattice-matched to GaSb substrates, the energy band gap varies between 1.7 μm and 4.3 μm . GaInAsSb materials are also of interest due to the miscibility gap with a critical temperature estimated to be 1467 °C. The nonequilibrium growth by metal-organic chemical vapour deposition (MOCVD) and molecular beam epitaxy (MBE) can overcome the difficulty of phase separation in the miscibility gap. The growth of quaternary GaInAsSb alloys has been reported by liquid phase epitaxy (LPE) [1, 2], MOCVD [3–5], MBE [6, 7] and liquid phase electroepitaxy (LPEE) [8, 9]. Photodiodes [5, 10–12] and lasers [13–15] fabricated from GaInAsSb materials have also been demonstrated. Most of the epitaxial growth of materials and the fabrication of devices were performed on the GaSb-rich end of the composition range. Pyramids and other defects were likely to occur on the surface of GaSb, GaSb-rich GaInSb and GaInAsSb epilayers. In this work, we report the growth of GaInAsSb alloys on GaSb substrates by MOCVD, with the composition of the films on the InAs-rich end and on the GaSb-rich end.

2. Experimental procedure

The epitaxial growth was performed in a horizontal, atmospheric MOCVD pressure reactor. The precursors were trimethylgallium (TMGa), trimethylindium

(TMIn), trimethylantimony (TMSb) and 10% arsine diluted by hydrogen. The source temperatures for TMGa, TMIn and TMSb were -12°C , 17°C , and -10°C , respectively. Pd-purified H_2 at a total flow of $3\text{--}5 \text{ l min}^{-1}$ was the carrier gas. (100)-oriented, Te-doped GaSb and high resistivity GaAs were used as substrates. The substrates were first cleaned by degreasing in organic solvents and deionized water. They were then chemically etched. For GaSb substrates, the etchant used was a mixed solution of nitric acid, hydrochloric acid and acetic acid ($\text{HNO}_3:\text{HCl}:\text{CH}_3\text{COOH} = 0.2:2:10$) for 10 min. The etchant for GaAs was the standard chemical etching solution ($\text{H}_2\text{SO}_4:\text{H}_2\text{O}:\text{H}_2\text{O}_2 = 5:1:1$). After etching, the substrates were rinsed with deionized water, blown dry with filtered nitrogen and loaded into the reaction chamber.

GaSb and GaAs substrates were protected from decomposing by TMSb and arsine sources before reaching growth temperature. The growth parameters, such as growth temperature, mole ratios of the input sources, were optimized to decrease the lattice mismatch between GaInAsSb epilayer and the GaSb substrate. Table I presents the optimized growth parameters of $\text{Ga}_{1-x}\text{In}_x\text{As}_y\text{Sb}_{1-y}$ grown on GaSb substrates. Under these conditions the solid compositions of the epilayers were on the InAs-rich end with $x > 0.7$, $y > 0.7$, and on the GaSb-rich end with $x < 0.3$, $y < 0.3$, as shown in Fig. 1. The thickness of the epilayers was about 1–3 μm .

The surface morphologies were examined by means of optical microscopy and scanning electron microscopy (SEM). The solid composition and lattice mismatch were measured by electron microprobe analysis and X-ray diffraction, respectively. X-ray diffraction was also used to evaluate the crystalline quality of

TABLE I Growth conditions of GaSb-rich and InAs-rich $\text{Ga}_{1-x}\text{In}_x\text{As}_y\text{Sb}_{1-y}$ films on GaSb substrates

Growth conditions	InAs-rich	GaSb-rich
Growth temperature ($^{\circ}\text{C}$)	570–620	570–640
TMGa flux (mol/min)	$(1-1.5) \times 10^{-6}$	$(2-10) \times 10^{-6}$
TMin flux (mol/min)	$(0.8-3) \times 10^{-5}$	$(2-5) \times 10^{-6}$
TMSb flux (mol/min)	$(0.8-3) \times 10^{-5}$	$(9-18) \times 10^{-6}$
AsH ₃ flux (mol/min)	$(3-5) \times 10^{-5}$	$(1-3) \times 10^{-6}$
III/V	0.2–0.4	0.4–1.3
Total H ₂ flux (l/min)	3	3–5

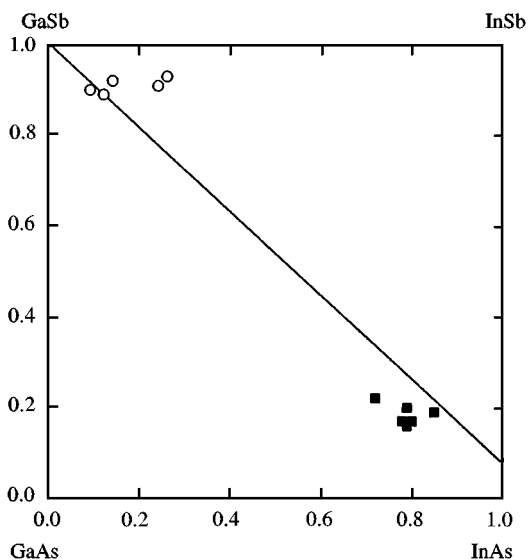


Figure 1 Solid phase field for $\text{Ga}_{1-x}\text{In}_x\text{As}_y\text{Sb}_{1-y}$ showing the solid compositions grown by MOCVD. The iso-lattice for GaSb substrate is also shown.

the epilayers. A standard Hall measurement was performed to determine the electrical properties of GaInAsSb epilayers grown on semi-insulating GaAs substrates.

3. Results and discussion

3.1. X-ray diffraction

GaSb-rich and InAs-rich GaInAsSb epilayers were grown on GaSb substrates. The growth parameters used are presented in Table I. Single crystal X-ray diffraction measurements were used to evaluate the lattice mismatch between the epilayer and substrate. Typical X-ray diffraction results for several samples of GaInAsSb/GaSb are shown in Fig. 2. The lattice mismatch between GaInAsSb and GaSb substrate was about 1–2%. A minimum mismatch of 0.4% was achieved.

3.2. Solid composition

The solid composition of GaInAsSb was dependent on growth temperature. Figs 3 and 4 show the temperature dependences of In composition x and As composition y , respectively. In Fig. 3, the GaInAsSb alloys were grown on GaSb substrates at temperatures between 570 and 640 $^{\circ}\text{C}$. Indium composition x

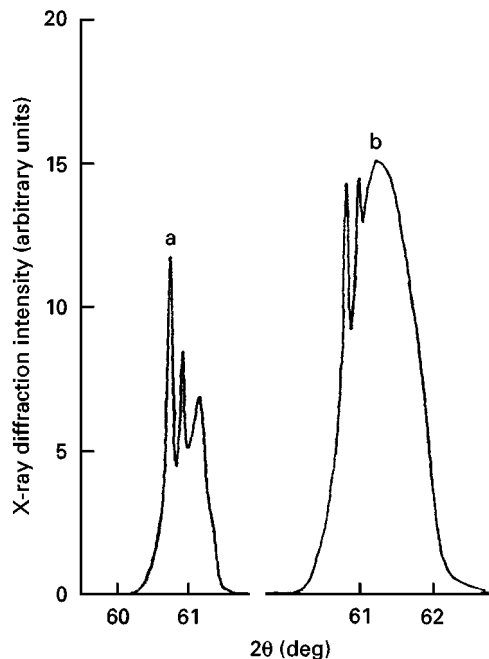


Figure 2 X-ray diffractions of GaSb-rich and InAs-rich $\text{Ga}_{1-x}\text{In}_x\text{As}_y\text{Sb}_{1-y}/\text{GaSb}$ samples (a) solid composition $x = 0.12$, $y = 0.11$, thickness $d = 1 \mu\text{m}$, (b) solid composition $x = 0.84$, $y = 0.81$, thickness $d = 3.5 \mu\text{m}$.

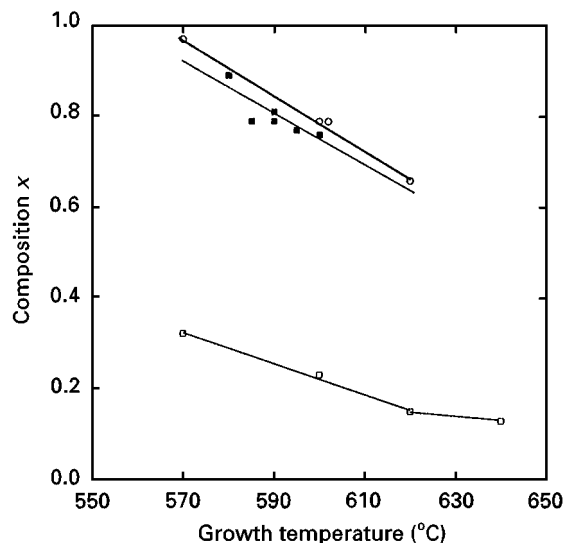


Figure 3 Solid composition x of $\text{Ga}_{1-x}\text{In}_x\text{As}_y\text{Sb}_{1-y}$ versus growth temperature, (○) III/V = 0.36, Ga/III = 0.07, Sb/V = 0.17, (■) III/V = 0.22, Ga/III = 0.13, Sb/V = 0.16, (□) III/V = 0.75, Ga/III = 0.80, Sb/V = 0.87.

decreased with increasing growth temperature. This phenomenon was often attributed to the difference of pyrolysis efficiency between TMGa and TMin. The pyrolysis temperature of TMGa was higher than that of TMin, which pyrolyses completely at 500 $^{\circ}\text{C}$ [16]. In the range 570–620 $^{\circ}\text{C}$, the pyrolysis efficiency of TMGa increased with increasing growth temperature, resulting in the decrease of indium composition in the epilayers. When the growth temperature is above 620 $^{\circ}\text{C}$, TMGa nearly completely pyrolysed. The rate of decrease of indium composition x was slowing.

Fig. 4 shows the unusual temperature dependences of As composition y in GaInAsSb alloys.

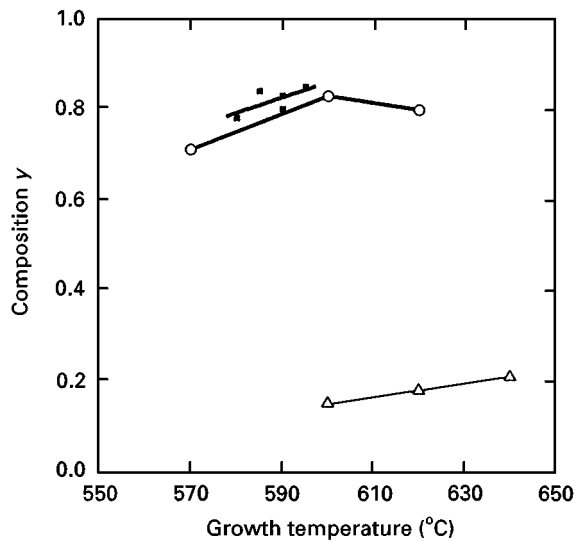


Figure 4 Solid composition y of $\text{Ga}_{1-x}\text{In}_x\text{As}_y\text{Sb}_{1-y}$ versus growth temperature, (■) III/V = 0.22, Ga/III = 0.13, Sb/V = 0.16, (○) III/V = 0.36, Ga/III = 0.07, Sb/V = 0.17, (△) III/V = 0.75, Ga/III = 0.80, Sb/V = 0.87.

For InAs-rich films, in the range 570–600°C, y increased with increasing growth temperature. It could be proposed that the different pyrolysis efficiency between TMSb and AsH₃ was attributed to the increase of y . It is well known that TMSb nearly completely pyrolyses above 500°C [3]. On the contrary, the pyrolysis of AsH₃ was not complete and increased with increasing growth temperature [17]. The real ratio of As and Sb in the vapour phase consequently increased, resulting in the increase of As composition y . Above 600°C, AsH₃ pyrolysed completely. The solid composition y decreased with increasing growth temperature. The reason for this tendency was not very clear. A possible explanation was that the decrease of y might be due to the stronger parasitic reaction between TMIn and AsH₃ in the vapour phase when the growth temperature was increased [18]. For GaSb-rich samples, As composition y increased with increasing growth temperature from 600°C to 640°C, contrary to the results for InAs-rich films. In the growth of GaSb-rich films, TMGa and TMSb were the major precursors in the vapour and solid phase. The Ga/III and Sb/V ratios were 0.8 and 0.85, respectively. The strength of chemical bonding between Ga and As was stronger than that between In and As. The small amount of elemental As was bound by elemental Ga of high concentration to restrain the parasitic reaction occurring between In and As. Most of the As atoms released by pyrolysis of the TMGa were incorporated with Ga into the epilayer. So with increasing growth temperature, the As composition y continued to increase. The concentration of the input reactants in the vapour phase played a major role in determining the corresponding solid composition in GaInAsSb films.

Fig. 5 shows the effect of the vapour Ga/III ratio on the solid composition in $\text{Ga}_{1-x}\text{In}_x\text{As}_y\text{Sb}_{1-y}$ alloy films. It can be seen that the solid composition x was nearly proportional to the vapour Ga/III ratio. The

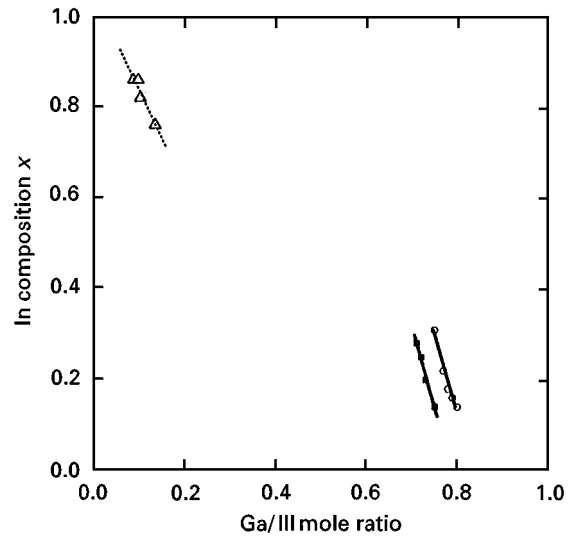


Figure 5 Solid composition x of $\text{Ga}_{1-x}\text{In}_x\text{As}_y\text{Sb}_{1-y}$ versus Ga/III ratio, (△) III/V = 0.23, Sb/V = 0.16, growth temperature $T = 600^\circ\text{C}$, (○) III/V = 0.75, Sb/V = 0.86, growth temperature $T = 600^\circ\text{C}$, (■) III/V = 0.23, Sb/V = 0.16, growth temperature $T = 620^\circ\text{C}$.

values of Ga distribution coefficient k_{Ga} , which was defined as $[(1-x)/x]/[(\text{Ga}/\text{In}) \text{ ratio}]$, were 1.48 at 620°C and 1.06 at 600°C for GaSb-rich epilayers, respectively. These data are in good agreement with the results reported by Bougnot *et al.* [5]. The increase of k_{Ga} with increasing growth temperature was in accordance with the variation of pyrolysis efficiency of TMGa and TMIn. For InAs-rich epitaxy, k_{Ga} at 600°C was about 2.

Fig. 6 shows the dependences of the As composition y on the Sb/V ratio for GaSb-rich and InAs-rich epilayers. The results reported by Fukui and Horikoshi [19] are also plotted in this figure. It was found that the composition y was nearly inversely proportional to the Sb/V ratio for the samples in the GaSb-rich corner. However, in the InAs-rich corner for Sb/V ratio between 0.1–0.3, the increase of composition y seemed slower than that of GaSb-rich films.

3.3. Surface morphology

The detailed surface morphology was examined using optical microscopy and scanning electron microscopy. Fig. 7 shows several surface observations of GaInAsSb samples. These observations demonstrated that the morphologies of InAs-rich GaInAsSb epilayers were very different from that of GaSb-rich GaInAsSb, as shown in Fig. 7. For GaSb-rich films, huge hillocks with a size of about 10 μm were observed on the surface. The pyramid-like hillocks had a rectangular base plane. The direction of the edges of the rectangular bottom was related to the tilt of the substrate. However, for InAs-rich samples, no such features were observed. The surface was mirror-like with very small hillocks on the surface. Such high quality surfaces with few pyramids would be beneficial for device fabrication. Previously reported results had shown that surface defects such as pyramids often occurred in the growth of antimonide compounds such as GaSb

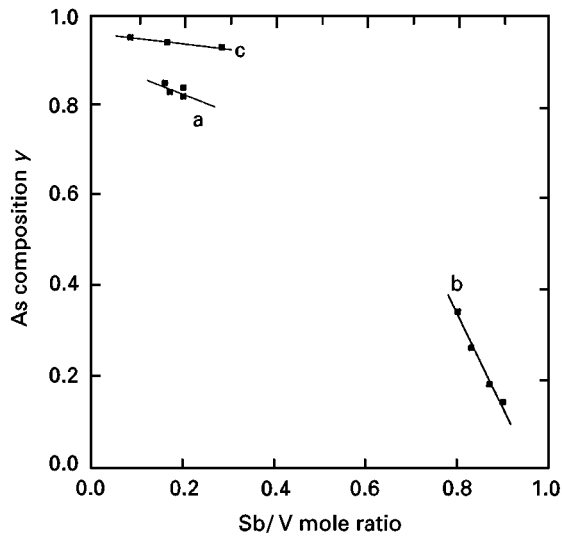


Figure 6 Solid composition, y of $\text{Ga}_{1-x}\text{In}_x\text{As}_y\text{Sb}_{1-y}$ versus Sb/V ratio, (a) III/V = 0.35, Ga/III = 0.06, $T = 600^\circ\text{C}$, (b) III/V = 0.75, Ga/III = 0.75, $T = 600^\circ\text{C}$, (c) results reported in [19].

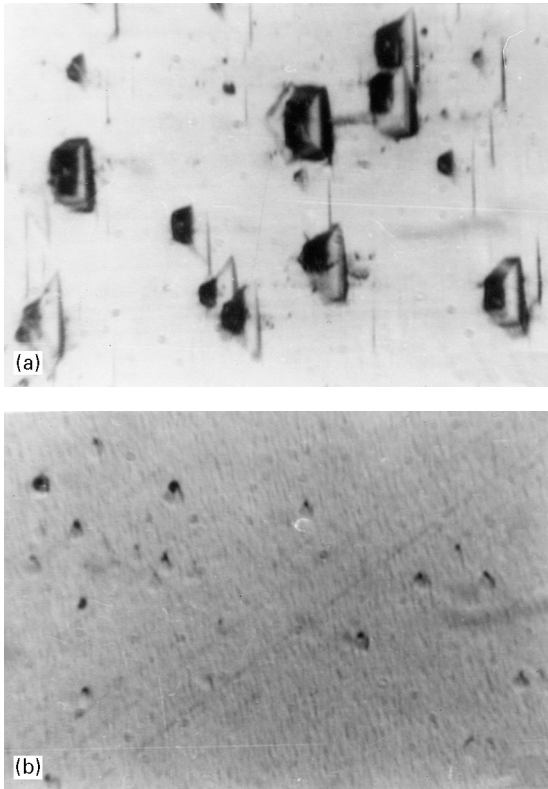


Figure 7 Surface morphologies of GaSb-rich and InAs-rich $\text{Ga}_{1-x}\text{In}_x\text{As}_y\text{Sb}_{1-y}$ /GaSb films, marker represents 10 μm (a) solid composition $x = 0.12$, $y = 0.11$, thickness $d = 1.5 \mu\text{m}$, lattice mismatch $\Delta a/a = 0.8\%$, (b) solid composition $x = 0.85$, $y = 0.81$, thickness $d = 1 \mu\text{m}$, lattice mismatch $\Delta a/a = 1.64\%$.

[20, 21], GaInSb [22] and GaInAsSb [5, 10]. In other material growth systems, such as GaAs, InP and GaInAs, no such features were observed. Considering the above results and the very different TMSb flux used for GaSb-rich and InAs-rich films, we believe that the presence of antimony was responsible for the occurrence of pyramids. For the growth of InAs-rich GaInAsSb films, the mole ratios of antimony versus group-V elements were chosen to be about 0.10–0.3

in our work, much lower than that for GaSb-rich GaInAsSb. In this case, the surface morphology of InAs-rich GaInAsSb epilayers was, to a large extent, determined by the incorporation of arsenic and group-III elements, avoiding the occurrence of hillocks.

3.4. Electrical properties

The electrical properties of unintentionally doped GaInAsSb deposited on semi-insulating GaAs substrates were measured using the Hall method, as presented in Table II. We observed that the type of conduction in InAs-rich film was n-type, whereas the conduction of GaSb-rich samples was p-type. A room temperature electron mobility of $5000 \text{ cm}^2 \text{ v}^{-1} \text{ s}^{-1}$ and an electron concentration of $3.6 \times 10^{17} \text{ cm}^{-3}$ for InAs-rich samples was obtained. For GaSb-rich films, the best results of hole mobility and hole concentration were $360 \text{ cm}^2 \text{ v}^{-1} \text{ s}^{-1}$ and $1 \times 10^{17} \text{ cm}^{-3}$, respectively. The origin of p-type conduction of GaSb-rich GaInAsSb alloys was often attributed to native lattice defects (i.e. Sb vacancies), antisite defects (Ga atoms at Sb sites), defect complexes ($\text{V}_{\text{Ga}}\text{Ga}_{\text{Sb}}$), or carbon impurities at Sb sites because the concentration of residual carbon was often of the order of 10^{17} – 10^{19} cm^{-3} . For InAs and InAsSb, the In–C bond was relatively weak and the result was n-type material with carbon on group-III sites [23]. This assumption could reasonably explain the n-type conduction of InAs-rich GaInAsSb in our work because the concentration of the In–C bond was much higher than that of the Ga–C bond.

According to our experimental results, we suggested that unintentionally doped GaInAsSb epilayer would show the lowest carrier concentration and the highest mobility when the effect of GaSb on the electrical conduction was comparable with that of InAs. This work is underway.

4. Conclusion

GaSb-rich and InAs-rich $\text{Ga}_{1-x}\text{In}_x\text{As}_y\text{Sb}_{1-y}$ layers were grown on GaSb substrates by atmospheric pressure MOCVD. The detailed surface morphology and electrical properties were investigated. The results demonstrated that the surface morphology of InAs-rich GaInAsSb epilayers was very different from that of GaSb-rich films. The Sb/V mole ratio in the vapour phase might result in this different surface feature. InAs-rich GaInAsSb epilayers showed n-type conduction, while GaSb-rich films were p-type. A reasonable

TABLE II Electrical properties of $\text{Ga}_{1-x}\text{In}_x\text{As}_y\text{Sb}_{1-y}$ films on GaAs substrates

x	y	$n(\text{cm}^{-3})$	$\mu_n(\text{cm}^2/\text{v.s.})$	$p(\text{cm}^{-3})$	$\mu_p(\text{cm}^2/\text{v.s.})$
0.93	0.76	3.6×10^{17}	5000		
0.92	0.75	4.5×10^{17}	4400		
0.90	0.76	7×10^{17}	2900		
0.14	0.08			1.1×10^{17}	360
0.26	0.07			1.1×10^{17}	320
0.24	0.08			1.6×10^{17}	110

explanation is that carbon impurity occupied different subsites due to the different strength of the Ga–C bond and the In–C bond.

Acknowledgements

The authors are grateful to Jingxiu Jiang, Naikang Liu and Zhongjiu Ge for their assistance in measurements. This work was supported by the National Advanced Material Committee of China under grant 863-715-01-02-02.

References

1. R. SANKARAN and G. A. ANTYPAS, *J. Cryst. Growth* **36** (1976) 98.
2. E. TOURNIE, F. PITARD and A. JOULLIE, *J. Cryst. Growth* **104** (1990) 683.
3. M. J. CHERNG, H. R. JEN, C. A. LARSEN and G. B. STRINGFELLOW, *J. Cryst. Growth* **77** (1986) 408.
4. M. J. CHERNG, G. B. STRINGFELLOW and R. M. COHEN, *Appl. Phys. Lett.* **64** (1984) 677.
5. G. BOUGNOT, F. DELANNOY, A. FOUCARAN, F. PASCAL, F. ROUMANILLE, P. GROSSE and J. BOUGNOT, *J. Electrochem. Soc.* **135** (1988) 1784.
6. W. T. TSANG, T. M. CHIU, D. W. KISKER and J. A. DITZENBERGER, *Appl. Phys. Lett.* **46** (1985) 283.
7. T. H. LIU, J. L. ZYSKIND and W. T. TSANG, *J. Electron. Mater.* **16** (1987) 57.
8. S. N. IYER, A. ABUL-FADL, A. T. MACRANDER, J. H. LEWIS, W. J. COLLIS and J. W. SULHOFF, *Mater. Res. Soc. Symp. Proc.* **160** (1990) 445.
9. S. IYER, S. HEGDE, K. K. BAJAJ, ALI ABDUL-FADL and W. MITCHEL, *J. Appl. Phys.* **73** (1993) 3958.
10. ZHOU TIANMING, ZHANG BAOLIN, JIN YIXIN, JIANG HONG and NING YONGQIANG, *Rare Metals* **11** (1992) 190.
11. A. K. SRIVASTAVA, J. C. DEWINTER, C. CANEAU, M. A. POLLACK and J. L. ZYSKIND, *Appl. Phys. Lett.* **48** (1986) 903.
12. J. E. BOWERS, A. K. SRIVASTAVA, C. A. BURRUS, J. C. DEWINTER, M. A. POLLACK and J. L. ZYSKIND, *Electron. Lett.* **22** (1986) 138.
13. H. K. CHOI and S. J. EGLASH, *Appl. Phys. Lett.* **61** (1992) 1154.
14. A. N. BARANOV, C. FOUILLANT, P. GRUNBERG, L. LAZZARI, S. GAILLARD and A. JOULLIE, *ibid.* **65** (1994) 616.
15. H. LEE, P. K. YORK, R. J. MENNA, R. U. MARTINELLI, D. E. GARBUZOR, S. Y. NARAYAN and J. C. CONNOLLY, *ibid.* **66** (1991) 1942.
16. C. A. LARSON and G. B. STRINGFELLOW, *J. Cryst. Growth* **75** (1986) 247.
17. G. B. STRINGFELLOW, *ibid.* **68** (1984) 111.
18. C. P. KUO, R. M. COHEN, K. L. FRY and G. B. STRINGFELLOW, *J. Electron. Mater.* **14** (1985) 231.
19. T. FUKUI and Y. HORIKOSHI, *Jpn. J. Appl. Phys.* **19** (1980) L53.
20. BAOLIN ZHANG, TIANMING ZHOU, HONG JIANG and YIXIN JIN, *Chemtronics* **5** (1991) 49.
21. F. PASCAL, F. DELANNEY, J. BOUGNOT, L. GOUSKOV, G. BOUGNOT, P. GROSSE and J. KAOUKAB, *J. Electron. Mater.* **19** (1990) 187.
22. ZHANG BAOLIN, ZHOU TIANMING, JIANG HONG, NING YONGQIANG, JIN YIXIN, HONG CHUNRONG and YUAN JINSHAN, *J. Cryst. Growth* **151** (1995) 21.
23. Z. M. FANG, K. Y. MA, R. M. COHEN and G. B. STRINGFELLOW, *Appl. Phys. Lett.* **59** (1991) 1446.

Received 23 June
and accepted 14 October 1997